PHYSICAL REVIEW C 72, 035207 (2005)

Target normal spin asymmetry of the elastic *ep* scattering at resonance energy

Dmitry Borisyuk and Alexander Kobushkin*
Bogolyubov Institute for Theoretical Physics Metrologicheskaya ulitsa 14-B, 03143, Kiev, Ukraine
(Received 31 May 2005; published 26 September 2005)

We study the target normal spin asymmetry for the reaction $ep \to ep$ at electron laboratory energy up to 2 GeV. The asymmetry is proportional to the imaginary part of the reaction scattering amplitude. To estimate the imaginary part of the amplitude we use the unitarity relation and saturate the intermediate hadron states by the proton and resonances from the first, second, and third resonance regions. The resonance electromagnetic transition amplitudes, which are needed to evaluate the asymmetry, are taken from experiment.

DOI: 10.1103/PhysRevC.72.035207 PACS number(s): 25.30.Bf, 13.88.+e, 14.20.Gk

I. INTRODUCTION

A study of elastic *ep* scattering is an important source of information about the internal structure of the proton. Because of the smallness of the fine-structure constant, $\alpha \approx 1/137$, the first-order perturbation term (the one-photon exchange) is assumed to give the main contribution to the electromagnetic transition amplitude. In the one-photon approximation the elastic *ep* scattering is described by two quantities, the electric $G_E(Q^2)$ and the magnetic $G_M(Q^2)$ form factors.

The form factors G_E and G_M are usually extracted from cross-section data by the Rosenbluth separation method. The database for G_E and G_M obtained by this method shows that the ratio G_E/G_M is approximately constant. Recently new precise measurements of the ratio G_E/G_M were done at Jefferson Lab [1–3] by the recoil polarization method [4,5] that yielded significantly different results from those of the Rosenbluth separation method [6].

Because both measurements are based on the one-photon exchange approximation it is natural to assume that this discrepancy may be explained by the second-order perturbation term in the α expansion. The α^2 perturbation term should result in many effects. Its real part contributes to the cross section and destroys the Rosenbluth formula. The imaginary part appears in one-particle polarization observables of the elastic *ep* scattering, the target and beam spin asymmetries, which vanish in the one-photon approximation. The present experimental technique makes it possible to measure such observables and thus to take under control effects beyond the one-photon approximation.

The aim of this paper is a calculation of the target normal spin asymmetry in the elastic *ep* scattering at electron laboratory energy $E_{\rm lab} \lesssim 2$ GeV.

The imaginary part of the scattering amplitude, which determines the asymmetry, is simply related (through the unitarity condition) to the electroproduction amplitudes of different hadronic states. The so-called "elastic" contribution (i.e., in which the hadronic intermediate state, entering the unitarity condition, is the proton) to the asymmetry was calculated in Ref. [7]. In Ref. [8] authors obtained strict bounds on the "inelastic" part of the asymmetry by using the Schwartz inequality. However, as the authors noted themselves, those bounds highly overestimate the actual values of the asymmetry, especially at high scattering angles.

In a recent work [9] the asymmetry was calculated with N and πN intermediate states. Such an approach gives a reasonable approximation at low electron energies, but becomes worse as the energy increases.

Contrary to [9], here we calculate the contribution of the resonances in the intermediate states, namely, $P_{33}(1232)$, $D_{13}(1520)$, $S_{11}(1535)$, $F_{15}(1680)$, and $P_{11}(1440)$, by using their experimental electroproduction amplitudes. Such an approach may be justified at intermediate energy, $E_{\rm lab} \lesssim 2$ GeV. For the large momentum-transfer region, Parton model calculations would be more adequate [10].

It was noted in Ref. [9] that the single-spin asymmetry is sensitive to electroproduction amplitudes in a wide range of photon virtualities, and this may be a new way of obtaining resonance transition form factors. The results of this work may be useful in the planning of such experiments.

The paper is organized as follows. In Sec. II we derive a general formalism for the asymmetry; in Secs. III and IV we explain how we describe the resonances and fit their electromagnetic transition amplitudes. Numerical results and conclusions are given Sec. V.

II. GENERAL FORMULAS

A. Notation

We denote the initial electron and proton momenta as k and P, respectively, and the final momenta as k' and P'. The transferred momentum is $q = k - k'$ ($q^2 < 0$), and the c.m. energy squared is $s = (P + k)^2 = (P' + k')^2$. Time and space components of four-momenta are denoted as $P = (\epsilon_P, \vec{P})$. M is the proton mass; the electron mass is neglected. We denote Dirac matrices as γ_μ and use the shorthand notation $\hat{a}$ for $a_\mu \gamma^\mu$.

Proton spinors with definite helicity λ and momentum P are

$$u_\lambda(P) = \begin{bmatrix} \sqrt{\epsilon_P + M}\, w_\lambda \\ \sqrt{\epsilon_P - M}(\vec{n}\vec{\sigma}) w_\lambda \end{bmatrix},$$

*Electronic address: kobushkin@bitp.kiev.ua

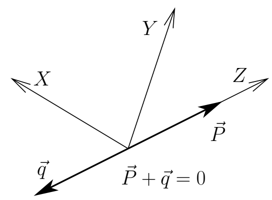

FIG. 1. Definition of transition amplitudes.

where

$$w_\lambda = \begin{bmatrix} e^{-i\varphi/2}\cos\frac{\theta+\pi(^1\!/_2-\lambda)}{2} \\ e^{i\varphi/2}\sin\frac{\theta+\pi(^1\!/_2-\lambda)}{2} \end{bmatrix}, \tag{1}$$

where θ and φ are spherical angles of the vector $\vec{n} = \vec{P}/|\vec{P}|$ and $\vec{\sigma}$ are Pauli matrices.

Electromagnetic current matrix elements for the proton read

$$\begin{aligned}\langle P'\lambda'|J^\mu|P\lambda\rangle &= \bar{u}_{\lambda'}(P')\Gamma^\mu u_\lambda(P) \\ &= \bar{u}_{\lambda'}(P')\left[2M(G_E-G_M)\frac{P_+^\mu}{P_+^2} + G_M\gamma^\mu\right]u_\lambda(P),\end{aligned} \tag{2}$$

where $|P\lambda\rangle$ is the proton state with momentum P and helicity λ, $P_+ = P + P'$, and $G_E \equiv G_E(q^2)$ and $G_M \equiv G_M(q^2)$ are the proton elastic form factors.

Current matrix elements between the proton (with momentum P) and other hadronic states (with momentum $P'' = P + q$) can be expressed by means of three independent invariant amplitudes. In the rest frame of the hadronic state (see Fig. 1) we have

$$\begin{aligned}\varepsilon_\mu^{(\lambda)}\langle h\Lambda|J^\mu|P^1\!/_2\rangle &= f_\lambda^{(h)}(q^2)\delta_{\Lambda,\lambda+1/2}, \\ \varepsilon_\mu^{(-\lambda)}\langle h-\Lambda|J^\mu|P-{}^1\!/_2\rangle &= \eta_h f_\lambda^{(h)}(q^2)\delta_{\Lambda,\lambda+^1\!/_2}.\end{aligned} \tag{3}$$

Here $\eta_h = \pi_h e^{i\pi(s_h-^1\!/_2)}$, h is some hadronic state, s_h and π_h are its spin and parity, respectively, and Λ is the spin projection onto the vector $\vec{P}$. The quantities $f_\lambda^{(h)}$ can be considered as helicity amplitudes of the process $\gamma^* p \to h$.

Polarization vectors of a virtual (spacelike) photon ε_μ are defined according to [11]. In the coordinate frame of Fig. 1 they are

$$\varepsilon_\mu^{(0)} = \frac{1}{\sqrt{-q^2}}(|\vec{q}\,|, 0, 0, -q^0), \qquad \varepsilon_\mu^{(\pm1)} = \frac{1}{\sqrt{2}}(0, \mp1, -i, 0), \tag{4}$$

where the superscript of ε shows the spin projection onto the z axis.

If the coordinate system is oriented arbitrarily, so that $\vec{n} = -\vec{q}/|\vec{q}\,| = (\cos\varphi\sin\theta, \sin\varphi\sin\theta, \cos\theta)$, then

$$\begin{aligned}\varepsilon_\mu^{(0)} &= \frac{1}{\sqrt{-q^2}}(|\vec{q}\,|, -q^0\vec{n}), \\ \varepsilon_\mu^{(\pm1)} &= \frac{1}{\sqrt{2}}(0, i\sin\varphi, -i\cos\varphi, 0) \\ &\quad \mp [(0, \cos\varphi\cos\theta, \sin\varphi\cos\theta, -\sin\theta)].\end{aligned} \tag{5}$$

Orthogonality relations

$$\sum_\lambda(-1)^\lambda\varepsilon_\mu^{(\lambda)}\overset{*}{\varepsilon}{}_\nu^{(\lambda)} = g_{\mu\nu} - \frac{q_\mu q_\nu}{q^2}, \quad g^{\mu\nu}\varepsilon_\mu^{(\lambda)}\overset{*}{\varepsilon}{}_\nu^{(\lambda')} = (-1)^\lambda\delta_{\lambda\lambda'}. \tag{6}$$

B. Asymmetry

The term "target normal asymmetry" corresponds to the situation in which the *target* proton is polarized along the *normal* to the reaction plane and other particles are unpolarized. Under such conditions the proton spin has two possible directions, say, above and below the reaction plane. Its invariant spin four-vector should be either collinear or anticollinear with the four-vector

$$S^\mu = \frac{2\varepsilon^{\nu\mu\sigma\tau}k_\nu P_\sigma P'_\tau}{\sqrt{-q^2[sq^2 + (s-M^2)^2]}}, \tag{7}$$

which is orthogonal to all momenta and satisfies $S^2 = -1$. The corresponding cross sections, $\sigma_\uparrow$ and $\sigma_\downarrow$, are equal in the one-photon approximation, so the difference between them is due to higher-order perturbative terms. The target normal asymmetry is defined as the dimensionless ratio

$$A_n = \frac{\sigma_\uparrow - \sigma_\downarrow}{\sigma_\uparrow + \sigma_\downarrow}. \tag{8}$$

The asymmetry is proportional to the imaginary part of the scattering amplitude. The imaginary part, in turn, can be expressed through the unitarity condition, which reads

$$i(T_{fi} - \overset{*}{T}_{if}) = \sum_n T_{fn}\overset{*}{T}_{in}, \tag{9}$$

where i and f are initial and final states, respectively, n is the so-called intermediate state, and T_{fi} are T-matrix elements. In our case we can, as the first approximation, use one-photon exchange amplitudes in the right-hand side of Eq. (9). Then we obtain

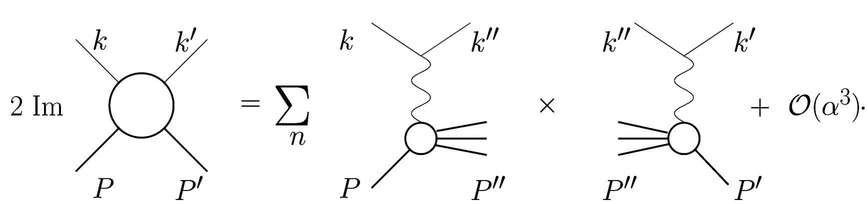

(10)

We denote $q_1 = k - k''$, $q_2 = k' - k''$, and the mass of hadronic intermediate state $W = \sqrt{P''^2}$.

As was shown in Ref. [8], with Eq. (10) and the time-reversal symmetry of the electromagnetic interaction, the asymmetry can be written as [12]

$$A_n = \frac{i\alpha q^2}{2\pi^2 D}\int_{M^2}^{s}\frac{s-W^2}{8s}dW^2\int d\Omega_{k''}\frac{1}{q_1^2 q_2^2}L^{\alpha\mu\nu} \times \sum_{\lambda_p,\lambda'_p} W_{\mu\nu}(P'\lambda'_p; P\lambda_p)\,\bar{u}_{\lambda_p}(P)(-\gamma^5\hat{S}\Gamma_\alpha)u_{\lambda'_p}(P') \quad (11)$$

in the first nonvanishing order of α, where Γ_α is defined in Eq. (2),

$$D = 4\left[\frac{(2s+q^2-2M^2)^2}{4M^2-q^2}\left(4M^2G_E^2 - q^2G_M^2\right) + q^2\left(4M^2G_E^2 + q^2G_M^2\right)\right], \quad (12)$$

$$L^{\alpha\mu\nu} = \mathrm{Tr}(\hat{k}'\gamma^\mu\hat{k}''\gamma^\nu\hat{k}\gamma^\alpha), \quad (13)$$

and the hadronic tensor $W_{\mu\nu}$ is defined as

$$W_{\mu\nu}(P'\lambda'_p; P\lambda_p) = \sum_h (2\pi)^4\delta(P+k-P''-k'') \times \langle P'\lambda'_p|J_\mu|h\rangle\langle h|J_\nu|P\lambda_p\rangle. \quad (14)$$

Here $|h\rangle$ are all possible hadronic states, which we refer to as "intermediate states." They can be N, πN, $\pi\pi N$, ηN, and so on. $\sum_h$ is the short-hand notation for

$$\sum_N\sum_{\text{spins}}\int\prod_{a=1}^{N}\frac{d^3p_a}{(2\pi)^3 2\epsilon_{p_a}}, \quad (15)$$

where N is the total number of particles and p_a are their momenta.

Now we express the hadronic tensor $W_{\mu\nu}$ through the electroproduction helicity amplitudes $f_\lambda^{(h)}$.

Consider this tensor in the rest frame of the hadronic state $|h\rangle$, i.e., at $\vec{P}'' = 0$. We choose a coordinate system such that both vectors $\vec{P}$ and $\vec{P}'$ lie in the yz plane (see Fig. 2) and the angle between them is β; $0 \leqslant \beta \leqslant \pi$.

The sum $\sum_h$ can be split into two parts: first, the sum over total angular momentum (=spin) projections, and second, the sum over all remaining quantum numbers, which we denote as $\sum_h{}'$. The behavior of the state $|h\rangle$ with respect to spatial rotation is completely described by its spin and spin projection and does not depend on any other quantum numbers. Thanks to this fact, the sum over spin projections can be done explicitly:

$$\begin{aligned} W_{\mu\nu}(P'\lambda'_p; P\lambda_p) &= {\sum_h}'\sum_{\Lambda''}(2\pi)^4\delta(P+q_1-P'') \\ &\quad\times\langle P'\lambda'_p|J_\mu|h\Lambda''(\vec{e}_z)\rangle\langle h\Lambda''(\vec{e}_z)|J_\nu|P\lambda_p\rangle \\ &= {\sum_h}'(2\pi)^4\delta(P+q_1-P'') \\ &\quad\times\sum_{\Lambda,\Lambda',\Lambda''}\langle P'\lambda'_p|J_\mu|n\Lambda'(\vec{P}')\rangle \\ &\quad\times\langle h\Lambda'(\vec{P}')|h\Lambda''(\vec{e}_z)\rangle\langle h\Lambda''(\vec{e}_z)|h\Lambda(\vec{P})\rangle \\ &\quad\times\langle h\Lambda(\vec{P})|J_\nu|P\lambda_p\rangle. \end{aligned} \quad (16)$$

Here $|h\Lambda(\vec{a})\rangle$ denotes the state with the spin projection onto vector $\vec{a}$ equal to Λ.

Wave functions of these states are related by Wigner D functions [11]:

$$\langle h\Lambda''(\vec{e}_z)|h\Lambda(\vec{P})\rangle = \overset{*}{\mathcal{D}}{}^{(s_h)}_{\Lambda\Lambda''}(\varphi,\theta,0), \quad (17)$$

where φ and θ are polar angles of the vector $\vec{P}$ and s_h is the spin of the state $|h\rangle$. Using Eq. (17) and properties of D functions, we have

$$\begin{aligned} &\sum_{\Lambda''}\langle h\Lambda'(\vec{P}')|h\Lambda''(\vec{e}_z)\rangle\langle h\Lambda''(\vec{e}_z)|h\Lambda(\vec{P})\rangle \\ &\quad = \sum_{\Lambda''}\mathcal{D}^{(s_h)}_{\Lambda'\Lambda''}\left(\frac{\pi}{2},\theta-\beta,0\right)\overset{*}{\mathcal{D}}{}^{(s_h)}_{\Lambda\Lambda''}\left(\frac{\pi}{2},\theta,0\right) \\ &\quad = \mathcal{D}^{(s_h)}_{\Lambda\Lambda'}(0,\beta,0). \end{aligned} \quad (18)$$

Using amplitude definition (3), we obtain

$$\begin{aligned} W_{\mu\nu}(P'\lambda'_p; P\lambda_p) &= \sum_{\lambda,\lambda'}(-1)^{\lambda+\lambda'}\varepsilon_{1\nu}^{(2\lambda_p\lambda)}\overset{*}{\varepsilon}{}_{2\mu}^{(2\lambda'_p\lambda')} \\ &\quad\times{\sum_h}'(2\pi)^4\delta(P+q_1-P'')f_\lambda^{(h)}\left(q_1^2\right)\overset{*}{f}{}_{\lambda'}^{(h)}\left(q_2^2\right) \\ &\quad\times\eta_h^{\lambda_p-\lambda'_p}\mathcal{D}^{(s_h)}_{\lambda_p(2\lambda+1),\lambda'_p(2\lambda'+1)}(0,\beta,0), \end{aligned} \quad (19)$$

where ε_1 and ε_2 are polarization vectors of the first (q_1) and second (q_2) photons of Eq. (10), defined according to Eqs. (5).

After that the asymmetry becomes

$$\begin{aligned} A_n &= \frac{\alpha q^2}{\pi D}\int_{M^2}^{s}\frac{s-W^2}{8s}dW^2\int d\Omega_{k''}\frac{1}{q_1^2q_2^2} \\ &\quad\times{\sum_h}'(2\pi)^3\delta(P+k-P''-k'') \\ &\quad\times\sum_{\lambda,\lambda'}f_\lambda^{(h)}\left(q_1^2\right)\overset{*}{f}{}_{\lambda'}^{(h)}\left(q_2^2\right)X_{\lambda\lambda'}^{(h)}\left(W,q_1^2,q_2^2\right), \end{aligned} \quad (20)$$

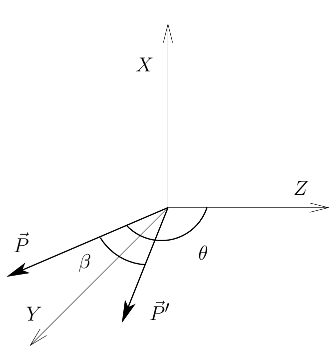

FIG. 2. Derivation of the hadronic tensor.

where

$$X^{(h)}_{\lambda\lambda'}\left(W, q_1^2, q_2^2\right) = i \sum_{\lambda_p,\lambda'_p} (-1)^{\lambda+\lambda'} \eta_h^{\lambda_p-\lambda'_p} \mathcal{D}^{(s_h)}_{\lambda_p(2\lambda+1),\lambda'_p(2\lambda'+1)}(0,\beta,0) \times L^{\alpha\mu\nu} \varepsilon_{1\nu}^{(2\lambda_p\lambda)} \overset{*}{\varepsilon}{}_{2\mu}^{(2\lambda'_p\lambda')} \bar{u}_{\lambda_p}(P)(-\gamma^5\hat{S}\Gamma_\alpha) u_{\lambda'_p}(P'). \quad (21)$$

The quantities $X^{(h)}_{\lambda\lambda'}$ can be calculated explicitly (provided the proton form factors are known), and the only unknowns in Eq. (20) are electromagnetic transition amplitudes $f^{(h)}_\lambda$.

III. THE MODEL FOR TRANSITION AMPLITUDES

Obviously it is practically impossible to take into account *all* allowed intermediate states. To proceed further, we need to restrict these states somehow. The authors of [9], for example, included only N and πN states. Although below the $\pi\pi N$ threshold ($E_{\rm lab} \approx 0.3$ GeV) such an approach gives an exact result, one can expect that, as the energy increases, this approximation becomes worse, as more intermediate states (e.g., ηN, $\pi\pi\pi N$) will be possible.

In this paper we use another way to model the intermediate states. We treat them as a number of resonances and neglect the nonresonant continuum contribution. At present we cannot estimate the nonresonant contribution well enough, but we can give a qualitative arguments that it is small.

At a glance one may conclude that the relative size of the nonresonant contribution will be approximately the same as in inelastic cross sections or structure functions. Actually it is likely to be much smaller for the following reason. Contrary to strictly positive quantities, such as cross sections, asymmetry can have either sign. Thus the contributions from different nonresonant states will mostly cancel each other. This is similar to the fact that the average of many uncorrelated random quantities has a much smaller dispersion than any of them.

At $P' = P$ the hadronic tensor $W_{\mu\nu}(P'\lambda'_p; P\lambda_p)$, which was introduced in previous section, turns into the hadronic tensor of inelastic *ep* scattering. It is natural to assume that the qualitative properties of both tensors are similar, so we should first look at what resonances contribute to the inelastic *ep* scattering.

There are three prominent resonant peaks in the inelastic *ep* cross section: the so-called first, second, and third resonance regions.

The first resonance peak is due to the Δ resonance [$P_{33}(1232)$], and the second peak consists of $D_{13}(1520)$ and $S_{11}(1535)$. There are many resonances that contribute to the third resonance region, but there are serious arguments (see, e.g., Ref. [13]) that the dominant contribution comes from $F_{15}(1680)$. Moreover, it is the only one for which the transition amplitudes are known. Although the Roper resonance $P_{11}(1440)$ does not contribute significantly to the inelastic *ep* scattering [13], we also include it in our calculations.

For the proton in the intermediate state we have

$$\sum_h{}' (2\pi)^3 \delta(P + q_1 - P'') = \int \frac{d^3P''}{2\epsilon_{P''}} \delta(P + q_1 - P'') = \delta(W^2 - M^2). \quad (22)$$

The resonance, however, has a mass $M_R \neq M$ and some finite width Γ_R, so we "spread" the δ function with the relativistic Breit-Wigner formula:

$$\delta\left(W^2 - M_R^2\right) \to \frac{\Gamma_R M_R}{\pi} \frac{1}{\left(W^2 - M_R^2\right)^2 + M_R^2\Gamma_R^2}. \quad (23)$$

After that the expression $\sum_h{}'(2\pi)^3\delta(P + q - P'') f^{(h)}(q_1^2) \overset{*}{f}{}^{(h)}(q_2^2)$, entering the formula for asymmetry, will take the form

$$f^{(p)}\left(q_1^2\right) \overset{*}{f}{}^{(p)}\left(q_2^2\right)\delta(W^2 - M^2) + \sum_R f^{(R)}\left(q_1^2\right) \overset{*}{f}{}^{(R)}\left(q_2^2\right) \times \frac{\Gamma_R M_R}{\pi} \frac{1}{\left(W^2 - M_R^2\right)^2 + M_R^2\Gamma_R^2}. \quad (24)$$

The first part is the "elastic" (proton) contribution; in the second part the sum runs over all resonances taken into account. The quantities $f^{(R)}$ depend only on q^2 but do not depend on W. They are related to commonly used [14] $A_{3/2}$, $A_{1/2}$, and $S_{1/2}$ as

$$f_1 = \kappa A_{3/2}, \quad \eta_R f_{-1} = \kappa A_{1/2},$$

and

$$f_0 = \frac{2q^2 M_R}{\sqrt{4M^2q^4 - q^2\left(M_R^2 - M^2 - q^2\right)^2}} \kappa S_{1/2}, \quad (25)$$

where $\kappa = \sqrt{\frac{M(M_R^2 - M^2)}{\pi\alpha}}$, whereas for the proton they are

$$f_1^{(p)}(q^2) \equiv 0, \quad f_0^{(p)}(q^2) = 2MG_E(q^2), \quad f_{-1}^{(p)}(q^2) = -G_M(q^2)\sqrt{-2q^2}, \quad (26)$$

which is easy to derive by a comparison of Eqs. (2) and (3).

For our calculation we use experimental data on A_H (i.e., $A_{3/2}$, $A_{1/2}$, $S_{1/2}$) given in [14]. Unfortunately, there are no data on $S_{1/2}$ for $D_{13}(1520)$ and $F_{15}(1680)$, so in our calculations we set it to zero.

To evaluate the asymmetry we need to fit these data somehow. The fitting procedure is described in the next section.

IV. FITTING PROCEDURE

Masses and widths of resonances were taken from the work of the Particle Data Group [15]. The proton form factors were modeled with the well-known dipole fit

$$G_M(q^2)/\mu_p = G_E(q^2) = \frac{1}{\left(1 + Q^2/Q_0^2\right)^2}, \quad (27)$$

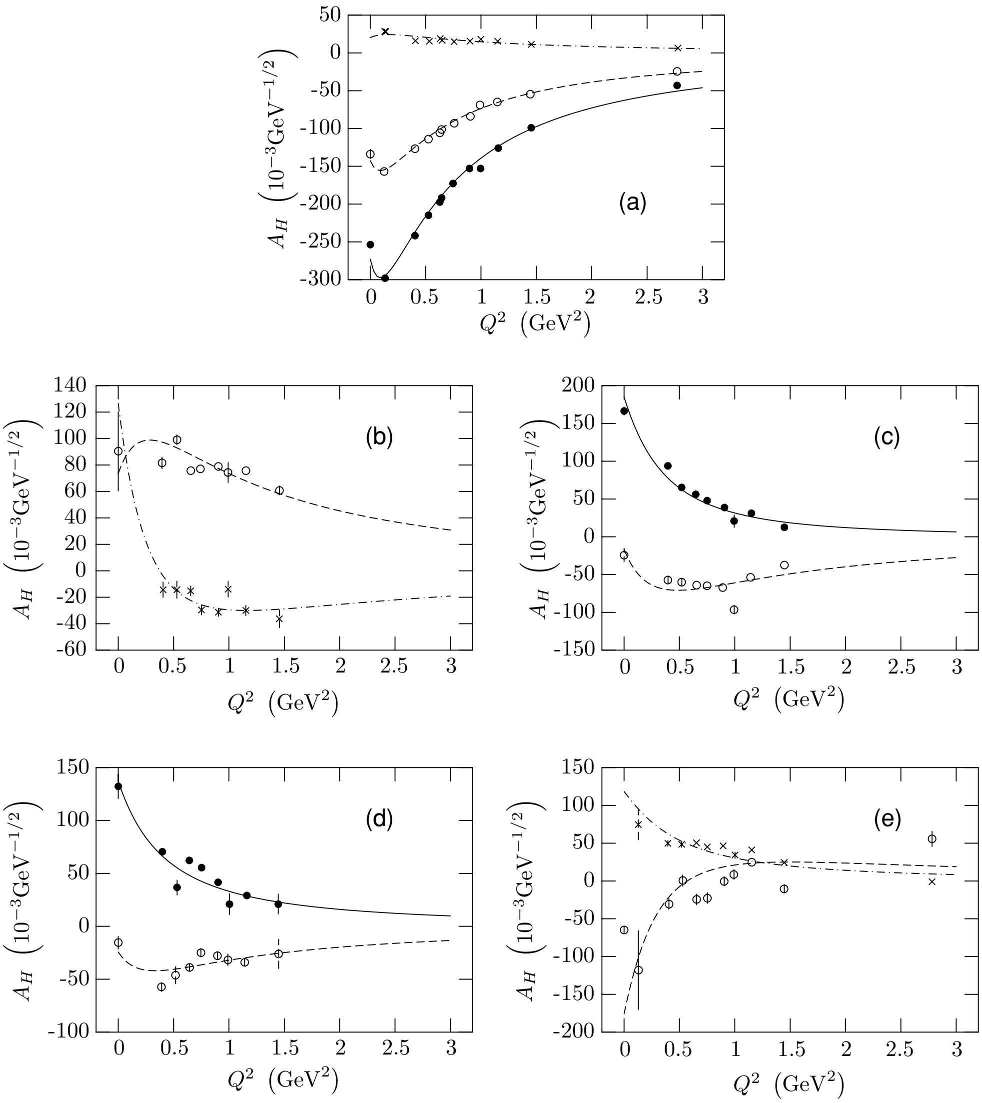

FIG. 3. Fit of the transition amplitudes $A_{3/2}$ (solid curves and filled circles), $A_{1/2}$ (dashed curves and open circles), and $S_{1/2}$ (dash-dotted curves and crosses) for resonances (a) $P_{33}(1232)$, (b) $S_{11}(1535)$, (c) $D_{13}(1520)$, (d) $F_{15}(1680)$ and (e) $P_{11}(1440)$. Experimental points are from a compilation of Ref. [14].

where $Q^2 \equiv -q^2$, $Q_0^2 = 0.71$ GeV^2, and $\mu_p \approx 2.79$ is the proton magnetic moment.

Now consider the fit of electroproduction amplitudes. According to quark model prediction, the high-Q^2 behavior of the transition amplitudes should be like $A_{1/2} \sim S_{1/2} \sim Q^{-3}$ and $A_{3/2} \sim Q^{-5}$ [16].

For the proton we have

$$A_{1/2} \sim \sqrt{-q^2}G_M(q^2) \sim \frac{Q}{\left(1 + Q^2/Q_0^2\right)^2} \sim Q^{-3}. \quad (28)$$

The denominator (dipole formula) is entirely due to quark structure, whereas the numerator is just a kinematical factor. However, the fact that $A_{1/2}$ tends to zero as $Q^2 \to 0$ is the specific feature of the proton. For the other hadronic states $A_{1/2}(0) \neq 0$, so, as in [16] and for the same reasons, we introduce the factor $\sqrt{(M_R - M)^2 + Q^2}$ and assume, instead of Eq. (28),

$$A_{1/2} \sim \frac{\sqrt{(M_R - M)^2 + Q^2}}{\left(1 + Q^2/Q_0^2\right)^2}. \quad (29)$$

So, to obtain correct asymptotic behavior of $A_{1/2}$ at $Q^2 \to 0$ and $Q^2 \to \infty$, it is useful to fit the function

$$\tilde{A}_{1/2} = \frac{\left(1 + Q^2/Q_0^2\right)^2}{\sqrt{(M_R - M)^2 + Q^2}} A_{1/2}, \quad (30)$$

which has finite values at both $Q^2 = 0$ and $Q^2 = \infty$. The same can be stated for $S_{1/2}$. On the other hand, $A_{3/2}$ has another asymptotic behavior ($\sim Q^{-5}$); therefore we could have used $(1 + Q^2/Q_0^2)^3$ instead of $(1 + Q^2/Q_0^2)^2$ in expressions (29) and (30) for $A_{3/2}$.

However, the Q^2 values needed for our calculation are not too high. Because $Q^2 = [(s - M^2)^2]/s \sin^2(\theta/2)$, where

θ is the c.m. scattering angle, we obtain $Q^2_{\max} \sim 3\,\text{GeV}^2$ at $E_{\text{lab}} = 2\,\text{GeV}$. Trying different parametrizations, we found that better agreement with the experimental data in the range $Q^2 \lesssim 3\,\text{GeV}^2$, especially for the δ resonance, is achieved if we use the same formulas,

$$A_H \sim \frac{\sqrt{(M_R - M)^2 + Q^2}}{\left(1 + Q^2/Q_0^2\right)^2}, \tag{31}$$

for all amplitudes. Thus we fit the functions

$$\tilde{A}_H = \frac{\left(1 + Q^2/Q_0^2\right)^2}{\sqrt{(M_R - M)^2 + Q^2}} A_H. \tag{32}$$

To describe high-Q^2 behavior better, we treat $\tilde{A}_H$ as a function of $\xi = 1 - [1/(1 + Q^2/Q_0^2)]$ instead of Q^2. At low Q^2 it does not matter, because $\xi \sim Q^2$, but the advantage is that ξ is finite at $Q^2 \to \infty$, so we can use a simple linear or polynomial fit for all ξ values.

In our calculations we restrict ourselves to the linear least-squares fit of the form

$$\tilde{A}_H(\xi) = a + b\xi. \tag{33}$$

Results of the fit are summarized in Table I. The corresponding dependence of amplitudes A_H versus Q^2 for all considered resonances is shown in Fig. 3 together with experimental points.

TABLE I. Fit of the transition amplitudes. All values are in inverse giga-electron-volts.

State	$\tilde{A}_{3/2}$	$\tilde{A}_{1/2}$	$\tilde{S}_{1/2}$
$P_{33}(1232)$	$-0.929 + 0.264\,\xi$	$-0.485 + 0.130\,\xi$	$0.069 + 0.022\,\xi$
$D_{13}(1520)$	$0.318 - 0.273\,\xi$	$-0.029 - 0.474\,\xi$	No data
$S_{11}(1535)$	0	$0.123 + 0.416\,\xi$	$0.212 - 0.614\,\xi$
$F_{15}(1680)$	$0.185 - 0.052\,\xi$	$-0.033 - 0.199\,\xi$	No data
$P_{11}(1440)$	0	$-0.351 + 0.787\,\xi$	$0.236 - 0.134\,\xi$

V. NUMERICAL RESULTS AND CONCLUDING REMARKS

Figure 4 displays the contribution of separate resonances to the target normal asymmetry A_n versus the c.m. scattering angle θ at different electron laboratory energies, E_{lab}. One sees that globally the $\Delta(1232)$ contribution is dominant. This is due to its large transition amplitudes in comparison with other resonances and the lowest mass among them. The contribution of the Roper resonance was obtained to be not negligible. Moreover at E_{lab} ~0.9 GeV it becomes comparable with the $\Delta(1232)$ contribution (the upper-right-hand panel of Fig. 4). This is a very nontrivial fact because the Roper contribution in inelastic eN scattering is very small. Nevertheless it can be studied in precise measurements of A_n under special kinematical conditions.

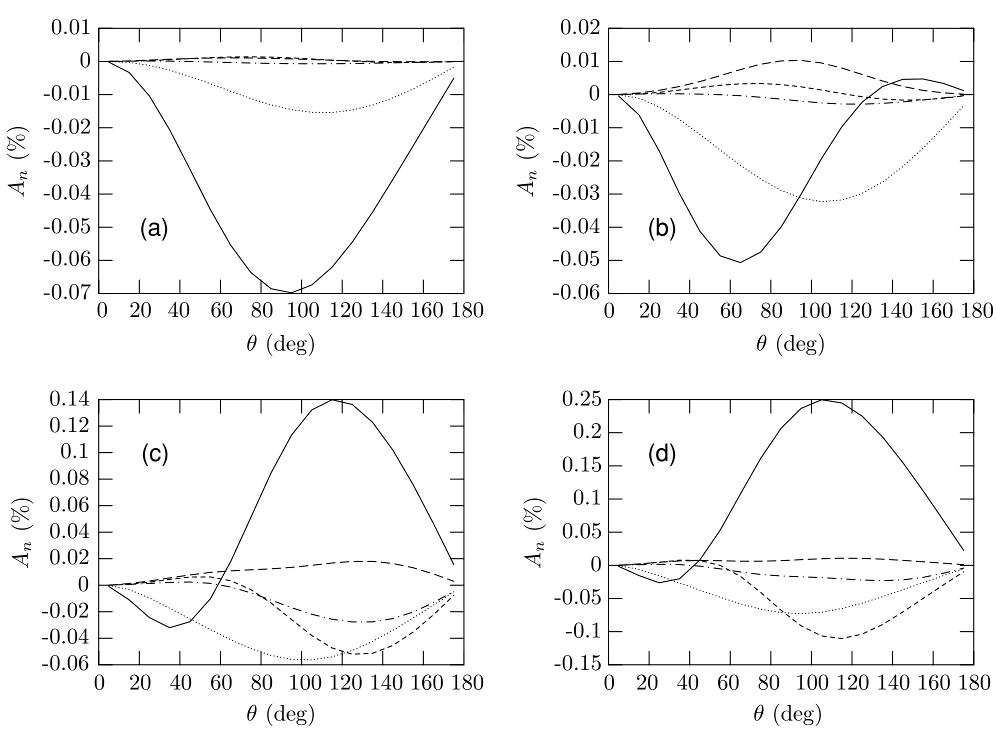

FIG. 4. The contribution of resonances to the asymmetry at different electron laboratory energies: (a) 0.57 GeV, (b) 0.855 GeV, (c) 1.4 GeV, (d), 2 GeV. Solid curves, $P_{33}(1232)$; long-dashed curves, $D_{13}(1520)$; short-dashed curves, $S_{11}(1535)$; dash-dotted curves, $F_{15}(1680)$; and dotted curves, $P_{11}(1440)$.

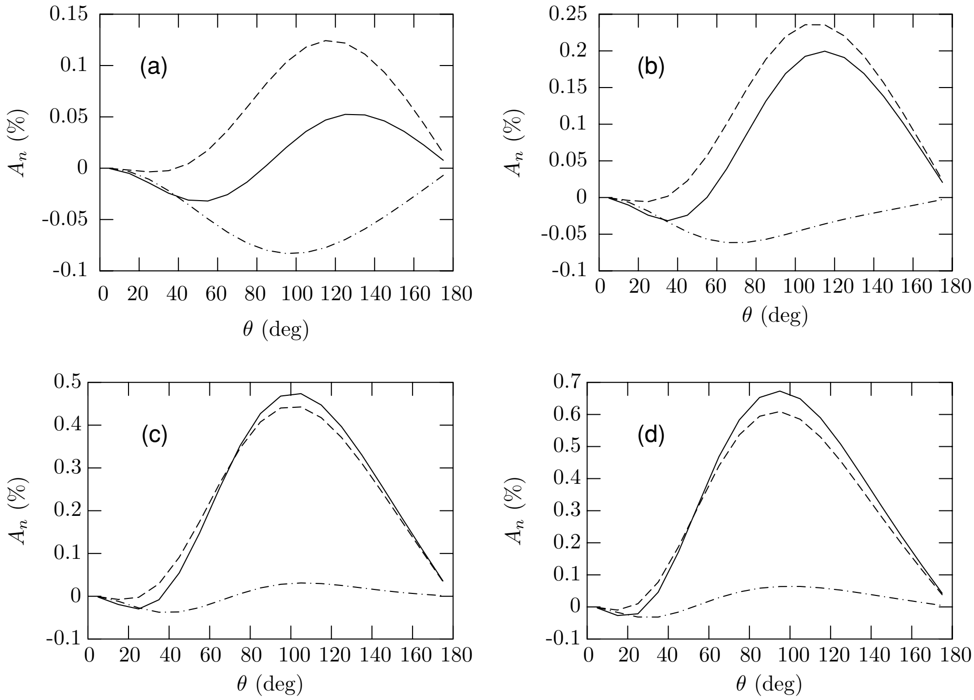

FIG. 5. Target normal spin asymmetry for different electron laboratory energies: (a) 0.57 GeV, (b) 0.855 GeV, (c) 1.4 GeV, (d) 2 GeV. The dashed curves are the elastic contributions, the dash-dotted curves are the inelastic contributions, and the solid curves are the totals.

One sees also that the contributions from the Δ and other resonances have mostly opposite signs and tend to cancel each other, especially at high beam energy. This is clearly seen from Fig. 5, in which we plot the elastic (proton) and inelastic (resonance) parts of the asymmetry and the total asymmetry. The elastic contribution dominates at low energies ($E_{\rm lab} <$ 0.3 GeV) and at energies higher than 1.3 GeV. It is quite obvious for the low energies, because the energy is insufficient for resonances to be produced. However, at high energies it is a nontrivial result that has interesting consequences. As was discussed in the introduction, the asymmetry depends on the imaginary part of the amplitude. However, because the real and imaginary parts are connected (by means of the dispersion relations), we may expect that the *real* part will also be defined mostly by proton contribution. This is important for the proper interpretation of the proton form-factor measurements.

In summary, we have calculated the target normal asymmetry A_n for the $e^- p \to e^- p$ reaction at the electron beam energy up to few giga-electron-volts. This quantity gives direct information on the imaginary part of the reaction scattering amplitude and comes from the second- and higher-order perturbative terms.

To calculate the imaginary part of the amplitude we used unitarity and saturated the intermediate hadron states by the proton (the so-called elastic contribution) and the resonances from the first, second, and third resonance regions (the inelastic contribution). We neglected the nonresonant inelastic contribution, which we expected to be small (see Sec. III). Besides that, the calculated contributions of separate resonances are interesting alone.

Our calculations demonstrate that, under special kinematical conditions (the electron laboratory energy near 0.9 GeV), the contribution of the Roper resonance $P_{11}(1440)$ becomes comparable with the Δ(1232) contribution and affects significantly the target asymmetry. It turn, this opens the possibility of studying $P_{11}(1440)$ electromagnetic transition amplitudes in precise measurements of the asymmetry.

[1] M. K. Jones *et al.*, Phys. Rev. Lett. **84**, 1398 (2000).
[2] O. Gayou *et al.*, Phys. Rev. Lett. **88**, 092301 (2002).
[3] V. Punjabi *et al.*, Phys. Rev. C **71**, 055202 (2005); Erratum-*ibid.*, **71**, 069902 (2005).
[4] A. I. Akhiezer and M. P. Rekalo, Dokl. Akad. Nauk SSSR **180**, 1081 (1968).
[5] A. I. Akhiezer and M. P. Rekalo, Sov. J. Part. Nucl. **4**, 277 (1974).
[6] J. Arrington, Phys. Rev. C **68**, 034325 (2003).
[7] A. J. G. Hey, Phys. Rev. D **3**, 1252 (1971).
[8] A. De Rujula, J. M. Kaplan, and E. de Rafael, Nucl. Phys. **B35**, 365 (1971).
[9] B. Pasquini and M. Vanderhaeghen, Phys. Rev. C **70**, 045206 (2004).
[10] Y. C. Chen, A. Afanasev, S. J. Brodsky, C. E. Carlson, and M. Vanderhaeghen, Phys. Rev. Lett. **93**, 122301 (2004).
[11] V. B. Berestetskii, E. M. Lifshitz, and L. P. Pitaevskii, *Relativistic quantum theory* (Pergamon, New York, 1971).
[12] There is a misprint in Eq. (2.18) of Ref. [8], a missing factor 8 in the denominator.
[13] P. Stoler, Phys. Rev. D **44**, 73 (1991).
[14] L. Tiator *et al.*, Eur. Phys. J. A **19**, 55 (2004).
[15] Particle Data Group, Phys. Lett. **B592**, 1 (2004).
[16] C. E. Carlson and N. C. Mukhopadhyay, Phys. Rev. Lett. **81**, 2646 (1998).